ACS APPLIED MATERIALS & INTERFACES

Research Article

Cite This: ACS Appl. Mater. Interfaces 2019, 11, 9621−9628

www.acsami.org

Robust Metallic Microcapsules: A Direct Path to New Multifunctional Materials

Dawei Sun,[†,‡] He Zhang,[§] Xin Zhang,[∥] and Jinglei Yang*[,†]

[†]Department of Mechanical and Aerospace Engineering, The Hong Kong University of Science and Technology, Kowloon 999077, Hong Kong SAR

[‡]College of Materials Science and Engineering, Beijing University of Technology, Beijing 100124, China

[§]Key Laboratory of Polymer Processing Engineering of the Ministry of Education, National Engineering Research Center of Novel Equipment for Polymer Processing, South China University of Technology, Guangzhou 510640, China

[∥]School of Civil and Environmental Engineering, Nanyang Technological University, 639798, Singapore

Supporting Information

ABSTRACT: Robustness of microcapsule shells determined the service life and application areas of final smart materials including self-healing composites, anticorrosion coatings, smart concretes, and so on. Herein, we designed and synthesized metal microcapsules by conducting electroless plating directly on liquid droplet surfaces, and metal shells showed superior stability in thermal (600 °C) and polar solvents (acetone and *N*,*N*-dimethylformamide) environments. More interestingly, the mechanical strength of metal shells was ten times higher than those of all published microcapsules. Besides, the smart epoxy composites remained stable mechanical properties with metal microcapsule concentrations, and this is the first time to report such results. For engineering materials, mechanical properties played an important role in practical applications, and a higher strength usually accompanied with better safety and longer service life. The microcapsules with designable structures could be synthesized by adjusting shell thickness and core fractions for practical requirements. The metal microcapsules had great potentials to be applied in a smart metallic matrix, conductive multifunctional materials, and pH-responsive materials. In addition, the electroless plating technique was also first applied to liquid surfaces pushing the development of novel smart materials.

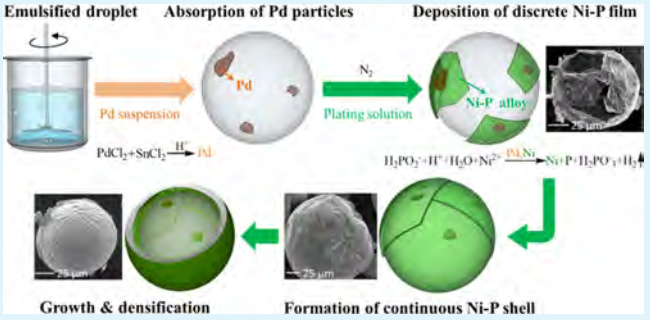

KEYWORDS: *metallic microcapsule, electroless plating, barrier property, robustness, multifunctional material*

1. INTRODUCTION

Microcapsules were utilized extensively in smart composites such as self-healing composites,[1−3] anticorrosion coatings,[4−10] and self-lubricating materials.[11,12] Although microcapsules brought "intelligent characters" to composites, they as the vulnerable components were easily attacked by such harsh surrounding environments as high temperatures, chemicals, and mechanical damages, resulting in the devastation of composites. Especially for such structural smart composites as epoxy resins, the matrix failure might cause serious safety and economy hazards. Boosting microcapsule robustness was an efficient way to extend the service life of smart composites. Traditional microcapsule shells were mainly made of polymer materials such as poly(urea-formaldehyde) (PUF) resin[13] or polyurea resin[4,14] and so on. Even some investigators applied glass bubbles as containers to load liquid agents.[15] However, the polymeric shells and deficient glass shells cannot survive long-termly in harsh conditions because the polymer shells were swelled easily by organic solvents,[16] resulting in the extraction of liquid cores, and the physical deficiencies within glass shells tended to leak liquid agents.[15] In addition, the mechanical properties of bulk composites were decreased significantly with microcapsule concentrations because of weak shell strength. Many publications tried to improve microcapsule shell robustness such as solvents resistance,[8,16,17] mechanical strength,[18,19] and thermal stability[17,20,21] through inorganic hybridization, cross-linking, and multiple-layered structures methods, respectively. Besides, some researchers tried to load liquid agents within inorganic silica shells[22,23] through sol−gel methods. However, the vulnerability of organic shell layers and the porosity of pure inorganic shell layers restricted the practical application of traditional microcapsules. It was highly necessary to develop new encapsulation techniques with stable and rigid shell structures.

Theoretically, metal materials were ideal candidates of microcapsule shell layers because of rigid and impermeable

Received: January 14, 2019
Accepted: February 7, 2019
Published: February 7, 2019

DOI: 10.1021/acsami.9b00827
ACS Appl. Mater. Interfaces 2019, 11, 9621−9628

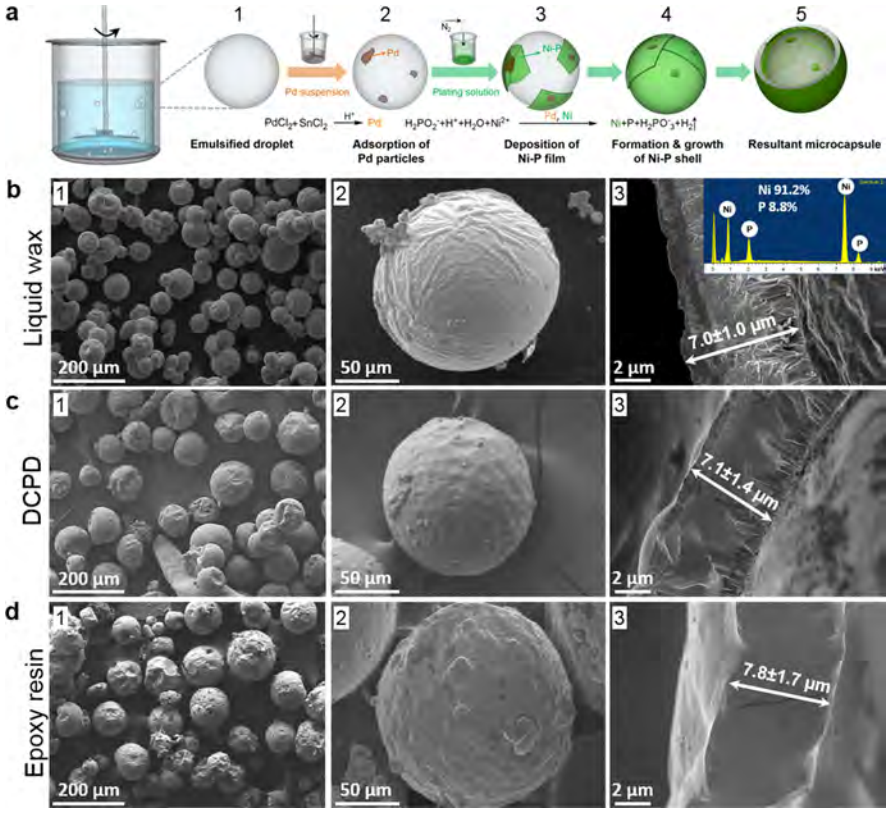

Figure 1. Schematic synthesis process and morphologies of typical metal microcapsules. (a) The overview of metal shell formation process: (a_1) a fresh emulsified microdroplet, (a_2) the reduced Pd nanoparticles were adsorbed on the surface of microdroplets via the Pickering effect, (a_3) the Ni^{2+} cations were reduced rapidly into a Ni membrane under the action of catalysts (Pd and Ni) at the initial stage of electroless plating, (a_4) the segmented Ni layer grew gradually along a droplet surface until complete mergence, followed by further thickening of the shell, and (a_5) the resultant microcapsule was obtained until complete reaction. The obtained microcapsules containing: (b) liquid wax, (c) DCPD, and (d) epoxy resin with (b_1, c_1, d_1) overview, (b_2, c_2, d_2) detailed surface morphology, and (b_3, c_3, d_3) shell profile indicating average thickness. The inset EDX spectrum in b_3 showed the metal shell contains 91.2% Ni and 8.8% P.

properties. In traditional situations, metal shells were usually fabricated through electroless plating techniques on particle surfaces such as polystyrene,[24] solid wax,[25] poly(*N*-isopropylacrylamide),[26] PMMA,[27] polycaprolactone,[27] and poly(L-lactide)[27] as protective metallic coatings. To prepare metal microcapsules with liquid cores, electroless plating techniques were conducted on the surfaces of microcapsules with polymelamine,[28] polyurea,[29] and PMMA[30] shells to obtain composite double-layered structures: inner-layered polymer shells and outer-layered metal shells. However, the inner-layered polymer shells isolate the thermal conduction between metal shells and phase change materials in thermal insulation applications and retard the release of healing agents from broken metal shells in self-healing applications.

Direct encapsulation of a liquid core played an important role in microcapsule-based smart materials[1,2] including self-healing and thermal insulation materials. However, there is a lack of fundamental understanding to grow directly metal shell on liquid droplet surfaces. In addition, the performance of metal shell microcapsules in epoxy matrix also needed to be investigated systematically.

In this study, we directly grew a metal layer around liquid droplets that adsorbed freshly reduced catalyst palladium (Pd) nanoparticles through the Pickering effect to activate electroless plating reaction in the Ni^{2+}-based solution. The Ni shell was electrolessly plated on various functional liquids to form novel microcapsules with unique thermal and mechanical features. In an epoxy composite, the Ni shell microcapsules will no longer weaken the matrix performance. This pioneering and promising approach will open a new window to develop novel multifunctional materials.[31−34]

2. RESULTS AND DISCUSSION

The schematic synthesis route was shown in Figure 1a. At 30 °C, oil microdroplets (Figure 1a_1) emulsion was dispersed well in the aqueous suspension containing freshly prepared Pd nanoparticles, which tended to adsorb on droplet surfaces (Figure 1a_2) by interfacial tension,[35] changing the emulsion appearance from white (Figure S1a, Supporting Information) to brown (Figure S1b, Supporting Information). The brown emulsion was then slowly added in nitrogen (N_2)-purged plating solution at 80 °C. The Ni^{2+} cations in solutions were reduced immediately into Ni upon contacting Pd nanoparticles on droplet surfaces, starting the formation of metal pieces. The fresh Ni was coated on liquid droplet surfaces and replaced Pd particles as a new catalyst to initiate the further growth of a shell layer around the droplet surfaces (Figure 1a_3 and Figure S2a, Supporting Information, showing the growing unmerged shell after reaction for 1 min) until all pieces met and merged together (Figure 1a_4 and Figure S2b, Supporting Information, illustrating a well-merged metal shell after reaction for 5 min). In addition, the interconnected pieces originating from scattered Pd particles were observed obviously as unsmooth joining scars (Figure S2b, Supporting Information). Metal

DOI: 10.1021/acsami.9b00827
ACS Appl. Mater. Interfaces 2019, 11, 9621−9628

shells were continuously thickening from around 200 nm (Figure S2c, Supporting Information) to around 1000 nm (Figure S2d, Supporting Information) with the increase of reaction duration from 1 to 5 min, respectively. After complete coverage of a metal membrane over a liquid droplet, the surfactant was introduced into the plating solution for subsequent dense growth of a metal shell by eliminating hydrogen bubbles on the external surfaces of a shell layer.[29] The reaction was stopped after 1 h, and final microcapsules (Figure 1a_5) were rinsed with deionized (DI) water and air-dried 12 h typically used for future characterizations unless otherwise specified.

The surface and shell morphologies of typical metal microcapsules were observed using field emission scanning electron microscopy (FESEM), as presented in Figure 1b,c,d (liquid wax, dicyclopentadiene (DCPD), and epoxy resin, respectively). Microscopic observations revealed highly similar features including well dispersibility (Figure 1b_1,c_1,d_1), external appearance (Figure 1b_2,c_2,d_2), and core−shell structure (Figure 1b_3,c_3,d_3) for all microcapsules. In addition, all shell walls (Figure 1b_3,c_3,d_3) had nearly uniform and dense thickness without visible voids or defects, indicating microcapsules with excellent stability in thermal and chemical environments (e.g., polar solvents). In addition, shell thickness was increased obviously under longer plating duration accompanied by the decrease of core fraction (Figure S3, Supporting Information) because of the deposition of more Ni. The metal shell was composed of 91.2% Ni and 8.8% phosphorus (P), as shown in the inset in energy dispersive X-ray (EDX) detector spectra in Figure 1b_3.

The surfactant played an important role in the formation of dense and well-dispersed metal microcapsules. When a liquid wax emulsion was added in the plating solutions, the droplets floated on the air−water interfaces of plating solutions, resulting in high concentrations and collision opportunities of microcapsules.[36] The microcapsules showed different performances in plating solution with or without NP-9 (surfactant), as shown in Figure S4a,b,c (Supporting Information).

In plating solution with NP-9, the final microcapsules were well spherical (Figure S4a_1, Supporting Information) while coalesced vigorously (Figure S4a_2, Supporting Information), even through holes were left within metal shells (Figure S4a_3, Supporting Information) after microcapsules being detached mechanically. The coalesced microcapsules were mainly resulted from the aggregation of unstable emulsion droplets during electroless plating process. In plating solution with nonionic surfactants, the superficial surfactants of emulsion droplets were replaced gradually by surrounding nonionic surfactants, resulting in the change of droplet curvature and instability of interfacial membranes.[37] The membranes were broken resulting in droplet coalescence along with Brownian movements (Figure 2a) with the formation of coalesced final microcapsules (Figure 2b) after plating process. In plating solution without NP-9, the emulsion droplets with hydrophilic surfaces were dispersed well on the surfaces of plating solutions (Figure 2c), resulting in well-dispersed metal microcapsules (Figure 2d). The liquid wax droplets with a stable interfacial membrane structure bounced back according to Derjaguin−Landau−Verwey−Overbeek theory when Brownian movements occurred, resulting in well-dispersed metal microcapsules (Figure S4c_1, Supporting Information). However, the nonionic surfactants showed different influence on

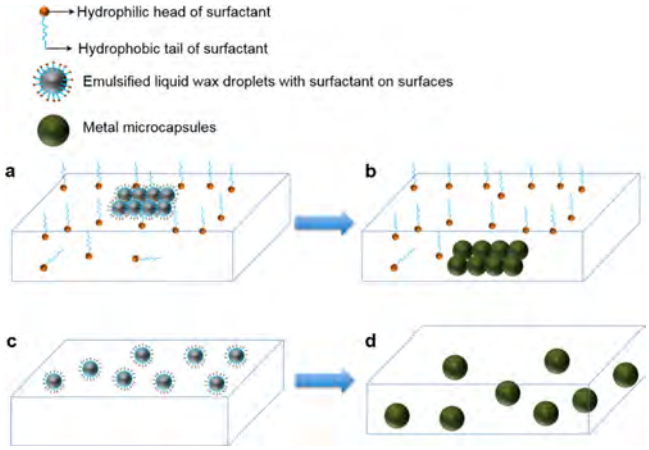

Figure 2. Influence of a surfactant on the dispersion status of metal microcapsules. (a) The emulsified liquid wax droplets with hydrophilic surface tend to coalesce together on the hydrophobic surface of plating solution and (b) the coalesced metal microcapsules were formed after electroless plating. (c) The emulsified liquid wax droplets with hydrophilic surface were dispersed well on the surface plating solution without surfactant and (d) the well-dispersed metal microcapsules were formed after electroless plating.

microcapsule shell structures. In plating solutions without surfactants, visible voids were observed on the surfaces (Figure S4c_2, Supporting Information) and cross section of metal shells (Figure S4c_2, Supporting Information). The newly produced hydrogen bubbles were absorbed on the outer surfaces of a metal shell, and they were hard to be removed and were trapped into voids with the growth of a metal shell. To prepare microcapsules with the optimum qualities, the liquid wax droplets were added first in plating solutions without surfactant to avoid coalescence. After 10 min, the surfactant was introduced in plating solution to remove hydrogen bubbles for subsequent dense growth of metal shell.[29] The well-dispersed and dense metal microcapsules were displayed in Figure S4b_1,b_2,b_3 (Supporting Information).

The thermal stability of metal microcapsules was evaluated through thermogravimetric analysis (TGA), and final curves were shown in Figure 3a as a function of temperature. All metallic shell materials maintained a constant weight before 500 °C followed by a slight tilting until 600 °C, presumably resulted from the oxidation of Ni by a trace amount of oxygen within N_2. Both pure DCPD and pure liquid wax were vaporized completely before 200 °C. However, encapsulated counterparts were released very gently until 500 °C because of the impermeability of metal shells in thermal environments. Besides impermeable shells, the baked microcapsules provided pretty similar morphologies with the fresh ones after 600 °C, as shown in Figure S5a,b (Supporting Information).

The core fraction was equal to the mass loss of metal microcapsules from room temperature to 500 °C, where metallic shell layers remained a constant weight. However, microcapsules containing an epoxy resin were heated, the sample weight was decreased vertically (Figure 3a), and debris was observed in the residual-baked samples (inset of Figure 3a). The main reason was due to the exorbitant inner pressure of damage-free microcapsules when epoxy resin was decomposed thermally into gas at 350 °C, resulting in the explosion of microcapsules. Therefore, the broken microcapsules containing an epoxy resin were tested to obtain core fraction instead of damage-free ones. In this way, the core fraction of

DOI: 10.1021/acsami.9b00827
ACS Appl. Mater. Interfaces 2019, 11, 9621−9628

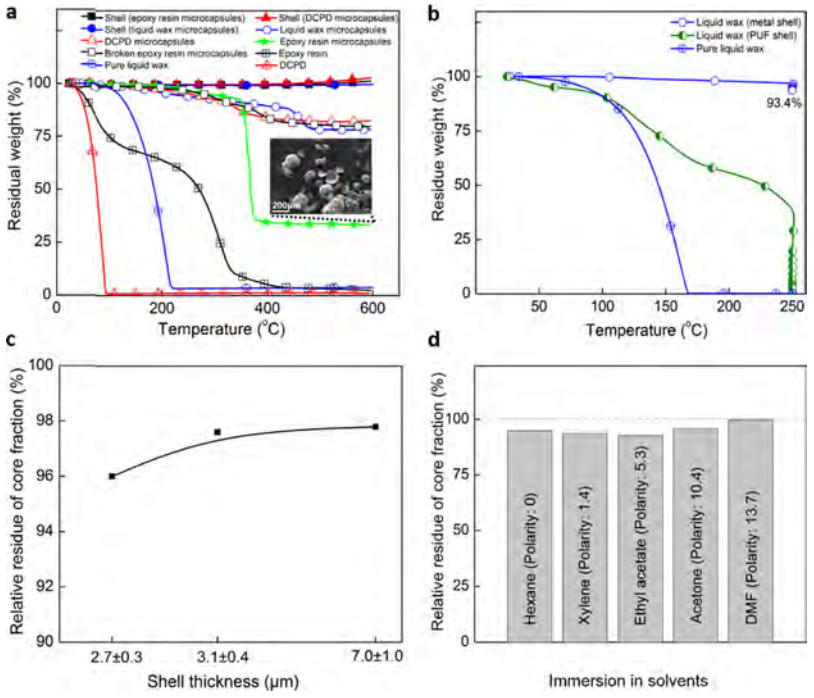

Figure 3. Thermal and chemical stability of metal microcapsules. (a) All samples including metal microcapsules, three types of microcapsule shells, and core materials were heated from room temperature to 600 °C at a rate of 10 °C/min in N_2 atmosphere. Shell debris was observed in the baked microcapsules containing an epoxy resin (inset of a). (b) Pure liquid wax, related metal microcapsules, and PUF microcapsules were heated from room temperature to 250 °C at a rate of 10 °C /min followed by isothermal for 60 min in N_2. (c) The relative residue of core fraction was plotted as a function of shell thickness, when microcapsules were stored in acetone for 5 days. (d) The relative residual core fraction was plotted as a function of solvents polarities, when metal microcapsules with a shell thickness of 2.7 ± 0.4 μm were immersed in organic solvents with different polarities for 5 days.

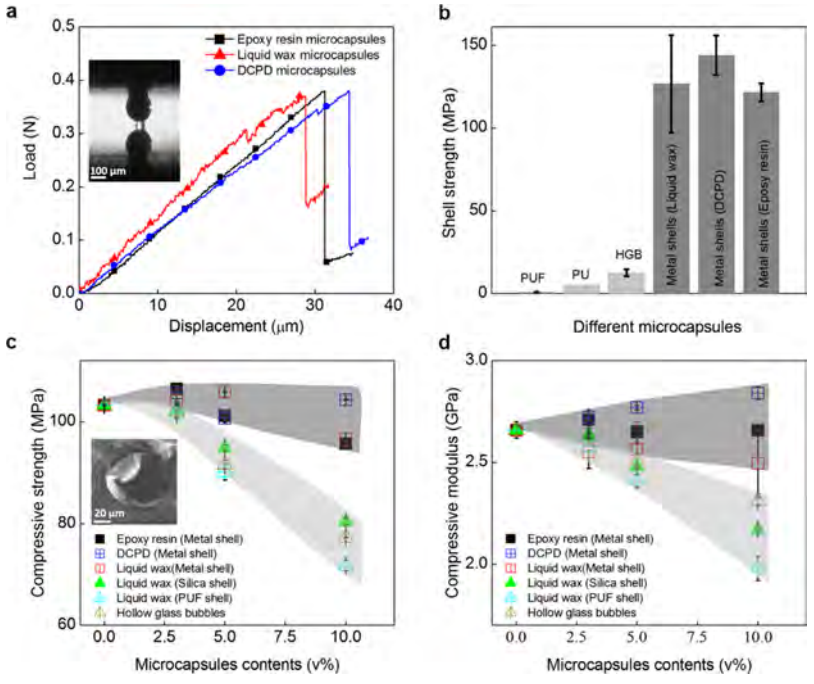

Figure 4. Mechanical properties of a single microcapsule and bulky composites. (a) The load−displacement curves of typical metal microcapsules containing liquid wax, DCPD, and epoxy resin, respectively. Liquid core was released after microcapsules being crashed (inset of a). (b) The normalized shell strength of metal microcapsules, PUF microcapsules, PU microcapsules, and HGB. Mechanical properties of composites were tested, when different microcapsules were dispersed in epoxy resin at different concentrations (0 v % to 3 v %, 5 v %, and 10 v %,). (c) The compressive strength of composites containing typical metal microcapsules, silica microcapsules, PUF microcapsules, and HGB. Microcapsules were ruptured by propagating cracks in composites (inset of c). (d) The compressive modulus of related composites containing different microcapsules with various concentrations.

DOI: 10.1021/acsami.9b00827
ACS Appl. Mater. Interfaces 2019, 11, 9621−9628

typical metal microcapsules containing liquid wax, DCPD, and epoxy resin was obtained as 21.3 wt % (71.6 vol %), 17.3 wt % (62.8 vol %), and 20 wt % (66.5 vol %), respectively. The volume percentage of core material was calculated according to eq S1 (Supporting Information).

To further investigate the isothermal stability of metal microcapsules, the samples (pure liquid wax, PUF microcapsules containing liquid wax, and metal microcapsules containing liquid wax) were stored in isothermal conditions (250 °C for 1 h) to observe the variation of core fractions and shell morphologies. As shown in Figure 3b, both pure liquid wax and that within PUF shells were evaporated fast and completely, but liquid wax encapsulated by a metal shell was reserved around 69% after isothermal process, because an impermeable metal shell trapped most liquid wax vapor. Besides, baked metal microcapsules (Figure S6a, Supporting Information) also remained a stable shape and morphologies after isothermal process (Figure S6b, Supporting Information) because of high melting point of Ni (1455 °C), whereas serious distortion occurred to PUF microcapsules (Figure S6c,d, Supporting Information). The microstructures of Ni−P alloy were amorphous when the phosphorous content was higher than 7 wt %.[38] The atom arrangement within Ni−P alloy is random and isotropy without obvious grain clearance and lattice defect.[39] The microstructures of Ni−P alloy still remained amorphous and dense under a higher temperature until 320 °C.[40] Unlike metal shells, PUF shells were decomposed upon a temperature exceeded 200 °C.[41]

To measure the viability in organic solvents, metal microcapsules with different shell thickness were immersed in acetone for 5 days to observe the variation of core fraction and morphologies. As shown in Figure 3c, residual core fractions of all metal microcapsules remained more than 96% of original values, indicating that the impermeability of microcapsules in acetone was influenced slightly by shell thickness. Besides, the residual metal microcapsules also showed a stable shape and appearance (Figure S6e,f, Supporting Information) after immersion in acetone. For comparison, the core fraction of PUF microcapsules was decreased to 0% after immersion, along with serious shrinkage of shapes from spherical (Figure S6g, Supporting Information) to irregular (Figure S6h, Supporting Information) because of poor stability of a PUF resin.[8] Additionally, the effect of solvent polarity on microcapsules stability was also investigated by immersing metal microcapsules in different organic solvents. The residual core fraction was shown in Figure 3d. For all cases, the relative residue of core fraction was higher than 93% resulting from the outstanding stability of a metal shell in various organic solvents. The amorphous microstructures of Ni−P alloy[38] were accompanied with the dense atom arrangement.[39] Both polar and nonpolar organic solvents molecules were hardly to penetrate Ni−P alloy without physical deficiencies because of weak compatibility. The impermeability of Ni−P alloy was influenced slightly by thickness.

Mechanical tests of a single microcapsule and bulky composites were conducted through a single microsphere compression apparatus[42] and Instron testing machine (ASTM D695), respectively. The representative load−displacement curves of all typical metal microcapsules were presented in Figure 4a with a diameter of 111.3 μm (liquid wax microcapsule), 132.5 μm (DCPD microcapsule), and 133.3 μm (epoxy resin microcapsule). All metal microcapsules responded similarly to external forces. The loads rose linearly with a displacement until the peak value, where microcapsules were crashed along with the leakage of a liquid core (inset of Figure 4a). The peak load and corresponding displacement of every metal microcapsule were maintained within 0.37−0.38 N and 28.8−34.4 μm, respectively.

The normalized shell strength, σ_{max}, was calculated as the following eq 1:

$$\sigma_{max} = \frac{P_{max}}{\pi\left[\left(\frac{D_0}{2}\right)^2 - \left(\frac{D_i}{2}\right)^2\right]} = \frac{P_{max}}{\pi t(D_0 - t)} \quad (1)$$

where P_{max} represents the peak load and D_0, D_i, and t are the outer diameter, inner diameter, and shell thickness of microcapsules, respectively. The normalized shell strength of all microcapsules including metal microcapsules and traditional microcapsules was shown in Figure 4b. Obviously, the metal microcapsules displayed the highest strength, ranging from 120 to 140 MPa. The shell strength of traditional PUF microcapsules,[42] polyurethane (PU) microcapsules,[43] and hollow glass bubbles (HGB)[15] was 0.8 ± 0.3, 5.3 ± 1.9, 12.5 ± 2.0 MPa, respectively, which were obtained from previous investigations. By comparison, the shell strength of metal microcapsules was ten times higher than those of all published results. The low porosity and amorphous microstructures of Ni−P alloy provided metal microcapsules higher strength and hardness than traditional ones prepared from polyurea, PUF, or glass as shell materials.

The mechanical properties of bulky composites containing metal microcapsules were characterized in terms of compressive strength and compressive modulus, as shown in Figure 4c,d, respectively, as well as those of other microcapsule-modified epoxy samples. As shown in Figure 4c, the compressive strength of composites containing metal microcapsules ranged from 96 to 106 MPa, showing a marginal change in comparison with that of pure epoxy samples (103 MPa). However, composites containing other microcapsules presented declining compressive strength from 103 to 72 MPa with higher concentrations. Other microcapsules had weak shell strength and therein resulting in a low compressive strength in composites.[15] Besides compressive strength, compressive modulus of bulky composites was also insensitive to metal microcapsule concentrations. As shown in Figure 4d, compressive modulus of composites stabilized within 2.5 to 2.8 GPa when metal microcapsules were embedded, whereas that of traditional composites decreased obviously from 2.7 to 2.0 GPa with the increase of microcapsule concentrations. The stable mechanical properties of composites containing metal microcapsules were due to the high rigidity of metal shells, and it was a great improvement for traditional systems. More interestingly, metal microcapsules were still broken by propagating cracks in composites to release functional agents. As shown in the inset picture of Figure 4c, the microcapsule debris was observed obviously in broken epoxy composites, providing great potentials to develop novel smart engineering materials with ideal strength.

3. CONCLUSIONS

Electroless plating was conducted successfully on liquid droplet surfaces to prepare metal microcapsules with controllable shell thickness. Final microcapsules survived well in harsh conditions. The shell strength of typical metal microcapsules

DOI: 10.1021/acsami.9b00827
ACS Appl. Mater. Interfaces 2019, 11, 9621−9628

was ten times higher than those of all published results, and the bulky composites remained relatively stable mechanical properties with the increase of microcapsule concentrations. Metal microcapsules provided great potentials in the development of novel smart material systems.

4. EXPERIMENTAL SECTION

The preparation of metal microcapsules was divided into three steps. Firstly, the liquid droplets were prepared through emulsification. Secondly, the catalyst Pd was absorbed on the surface of liquid droplets by the Pickering effect. Finally, the metal shell was grown on the surface of liquid droplets to finish encapsulation.

4.1. Materials. Gum arabic, palladium chloride ($PdCl_2$), stannous chloride ($SnCl_2$), acetone, nickel sulfate, sodium hypophosphite monohydrate, sodium acetate, malic acid, lactic acid, thiourea, Tergitol (NP-9), xylene, and aqueous ammonia (28%) solutions were all purchased from Sigma-Aldrich without further purification. Liquid wax (Epolam), epoxy resin (Epolam 5015), and hardener 5014 were all purchased from Epolam Company. DCPD was purchased from Dow Chemicals.

4.2. Microcapsules Fabrication. *4.2.1. Preparation of Oil Microdroplets.* Gum arabic (0.75 g) as a surfactant was dissolved in 30 mL of DI water at 30 °C. Subsequently, 5g of oil phase (liquid wax, DCPD, or epoxy resin) was added in the surfactant solution under an agitation rate of 1250 rpm and allowed to stabilize for another 15 min. Finally, microdroplet solutions were washed with DI water for five times. Pure epoxy resin was diluted by xylene at a concentration of 90 wt %.

4.2.2. Adsorption of Pd on the Surfaces of Microdroplets. $PdCl_2$ (0.025 g) was dissolved in a 50 mL beaker containing 5 mL of concentrated HCl solution (36 wt %), and the beaker was suspended in a water bath with a temperature of 30 °C on a magnetic stirring apparatus. After complete dissolution of $PdCl_2$, 0.065 g of $SnCl_2$ was added and allowed to react for 10 min to obtain Pd particle suspension, which was subsequently mixed well with microdroplet solutions under a mechanical agitation of 200 rpm. After 10 min, the oil droplets with Pd on surfaces were washed for several times for future electroless plating process.

4.2.3. Encapsulation of Liquid Droplets through Electroless Plating. The plating solution was prepared by dissolving 3.0 g of nickel sulfate, 2.5 g of sodium hypophosphite monohydrate, 2.0 g of sodium acetate, 0.4 g of malic acid, 2.0 mL of lactic acid, and 10 droplets of thiourea solutions (0.01 wt %) in 100 mL of DI water. The pH value of plating solution was adjusted to 4.8 with ammonia solution. After the N_2-purged plating solution was heated to 80 °C, the microdroplets containing Pd particles were introduced dropwisely. The reaction proceeded first for 5 min followed by the addition of one droplet of NP-9. Then, electroless plating reaction was allowed to continue for another 55 min with the formation of typical metal microcapsules. Finally, the microcapsules were rinsed and washed with DI water for several times for future characterization after dry. In addition, the metal microcapsules containing liquid wax with different shell thickness (2.7 ± 0.3, 3.1 ± 0.4, and 7.0 ± 1.0 μm) were prepared by adjusting the plating duration (15, 30, and 60 min).

4.3. Characterization Methods. The microcapsules were characterized by FESEM (Joel, Model: JSM-7600F), EDX, and TGA.

4.3.1. Thermal Performances of Resultant Microcapsules. The thermal stability of metallic microcapsules was tested by thermogravimetric analysis (TGA, Q500) and characterized in terms of core fraction and morphology. Samples (10−20 mg) including typical metallic microcapsules (liquid wax microcapsules, DCPD microcapsules, epoxy resin microcapsules, and broken epoxy resin microcapsules), three types of core material, and related shell materials were heated from room temperature to 600 °C at a rate of 10 °C /min in N_2.

To test the isothermal stability of metallic microcapsules, typical metallic microcapsules, PUF microcapsules, and pure liquid wax were heated from room temperature to 250 °C at a rate of 10 °C/min followed by 60 min isothermal within N_2. Both metallic microcapsules and PUF microcapsules contained liquid wax as a core.

4.3.2. Robustness of Metallic Microcapsules in Organic Solvents. The robustness of metallic microcapsules in organic solvents was tested by immersing metallic microcapsules with different shell thickness (2.7 ± 0.3, 3.1 ± 0.4, and 7.0 ± 1.0 μm) in acetone at a concentration of 1.0 wt % for 5 days and characterized in terms of residual core fraction and shell morphologies. The robustness of PUF microcapsules was also tested for comparison. Both typical metallic microcapsules and PUF microcapsules contained liquid wax as a core.

In addition, the influence of solvent polarity on the robustness of microcapsules was also investigated. Metallic microcapsules with a shell thickness of 2.7 ± 0.4 μm were immersed in various organic solvents at a concentration of 1.0 wt % for 5 days and characterized in terms of the relative residue of core fraction. The applied organic solvents included hexane (polarity: 0), xylene (polarity: 1.4), ethyl acetate (polarity: 5.3), acetone (polarity: 10.4), and DMF (polarity: 13.7).

4.3.3. Mechanical Properties of Metallic Microcapsules. 4.3.3.1. Mechanical Characterization of Single Microcapsule. The mechanical property of a single typical metal shell microcapsule was analyzed through a single microsphere compression apparatus designed by previous investigations. The applied loading rate for a stepper actuator (Physik Instrumente-230S) was 2 μm/s controlled by computer. The load was recorded by a 2N load cell (FUTEK). Before test, images needed to be taken to measure the diameter of the metallic microcapsules. About 10 microcapsules of each type were tested, and the mean and standard errors were calculated.

4.3.3.2. Preparation and Mechanical Characterization of Composites. Epolam 5015 and hardener 5014 were firstly mixed uniformly according to a recommended weight ratio (3:1) followed by degassing for 20 min to remove trapped air bubbles. After the epoxy resin was precured for 3 h at room temperature, typical metallic microcapsules were introduced at different concentrations by volume from 0 vol % to 3 vol %, 5 vol %, and 10 vol % and then fabricated into compressive samples according to ASTM D695. The compressive samples were first cured for 24 h at room temperature and then post-cured for 16 h at 80 °C. Besides, the samples containing PUF microcapsules, silica shell microcapsules, and hollow glass bubbles were also prepared based on the same procedure. The compressive test was conducted using an Instron machine (Instron 5500R) with a loading speed of 1 mm/min to obtain compressive strength and compressive modulus. The broken samples could be observed through FESEM.

■ ASSOCIATED CONTENT

Supporting Information

The Supporting Information is available free of charge on the ACS Publications website at DOI: 10.1021/acsami.9b00827.

Schematic representation and pictures of the emulsion with catalyst, shell thickness variation and morphologies of microcapsules in plating solutions without surfactants, and morphologies of microcapsules after thermal treatment or chemical immersion (PDF)

■ AUTHOR INFORMATION

Corresponding Author

*E-mail: maeyang@ust.hk. Tel: +852 3469 2298.

ORCID

He Zhang: 0000-0001-7864-0305

Jinglei Yang: 0000-0002-9413-9016

Author Contributions

J.Y. and D.S. conceived and designed the study. D.S. performed the experiments and wrote the paper. H.Z. and X.Z. tested the mechanical strength of microcapsules and bulk

DOI: 10.1021/acsami.9b00827
ACS Appl. Mater. Interfaces 2019, 11, 9621−9628

composites. All authors commented and improved the manuscript.

Notes

The authors declare no competing financial interest.

■ ACKNOWLEDGMENTS

This work was supported by the Startup Fund from HKUST (grant no. R9365).

■ REFERENCES

(1) White, S. R.; Sottos, N. R.; Geubelle, P. H.; Moore, J. S.; Kessler, M. R.; Sriram, S. R.; Brown, E. N.; Viswanathan, S. Autonomic Healing of Polymer Composites. *Nature* **2001**, *409*, 794−797.
(2) Diesendruck, C. E.; Sottos, N. R.; Moore, J. S.; White, S. R. Biomimetic Self-Healing. *Angew. Chem., Int. Ed.* **2015**, *54*, 10428−10447.
(3) Coope, T. S.; Mayer, U. F. J.; Wass, D. F.; Trask, R. S.; Bond, I. P. Self-Healing of an Epoxy Resin Using Scandium(III) Triflate as a Catalytic Curing Agent. *Adv. Funct. Mater.* **2011**, *21*, 4624−4631.
(4) Cho, S. H.; White, S. R.; Braun, P. V. Self-Healing Polymer Coatings. *Adv. Mater.* **2009**, *21*, 645−649.
(5) Li, G. L.; Zheng, Z.; Möhwald, H.; Shchukin, D. G. Silica/Polymer Double-Walled Hybrid Nanotubes: Synthesis and Application as Stimuli-Responsive Nanocontainers in Self-Healing Coatings. *ACS Nano* **2013**, *7*, 2470−2478.
(6) Fu, J. J.; Chen, T.; Wang, M. D.; Yang, N. W.; Li, S. N.; Wang, Y.; Liu, X. D. Acid and Alkaline Dual Stimuli-Responsive Mechanized Hollow Mesoporous Silica Nanoparticles as Smart Nanocontainers for Intelligent Anticorrosion Coatings. *ACS Nano* **2013**, *7*, 11397−11408.
(7) Borisova, D.; Akçakayiran, D.; Schenderlein, M.; Möhwald, H.; Shchukin, D. G. Nanocontainer-Based Anticorrosive Coatings: Effect of the Container Size on the Self-Healing Performance. *Adv. Funct. Mater.* **2013**, *23*, 3799−3812.
(8) Wu, G.; An, J.; Tang, X.-Z.; Xiang, Y.; Yang, J. A Versatile Approach towards Multifunctional Robust Microcapsules with Tunable, Restorable, and Solvent-Proof Superhydrophobicity for Self-Healing and Self-Cleaning Coatings. *Adv. Funct. Mater.* **2014**, *24*, 6751−6761.
(9) Zhang, H.; Zhang, X.; Bao, C.; Li, X.; Sun, D.; Duan, F.; Friedrich, K.; Yang, J. Direct microencapsulation of pure polyamine by integrating microfluidic emulsion and interfacial polymerization for practical self-healing materials. *J. Mater. Chem. A* **2018**, *6* (47), 24092−24099.
(10) Zhang, H.; Yang, J. Etched glass bubble as robust microcontainer for self-healing materials. *J. Mater. Chem. A* **2013**, *1*, 12715−12720.
(11) Khun, N. W.; Zhang, H.; Tang, X.-z.; Yue, C. Y.; Yang, J. Short Carbon Fiber-Reinforced Epoxy Tribomaterials Self-Lubricated by Wax Containing Microcapsules. *J. Appl. Mech.* **2014**, *81*, 121004.
(12) Khun, N. W.; Sun, D. W.; Huang, M. X.; Yang, J. L.; Yue, C. Y. Wear Resistant Epoxy Composites with Diisocyanate-based Self-healing Functionality. *Wear* **2014**, *313*, 19−28.
(13) Brown, E. N.; Kessler, M. R.; Sottos, N. R.; White, S. R. In Situ Poly(urea-formaldehyde) Microencapsulation of Dicyclopentadiene. *J. Microencapsulation* **2003**, *20*, 719−730.
(14) Zhang, H.; Zhang, X.; Chen, Q.; Li, X.; Wang, P.; Yang, E.-H.; Duan, F.; Gong, X.; Zhang, Z.; Yang, J. Encapsulation of shear thickening fluid as easy-to-apply impact resistant material. *J. Mater. Chem. A* **2017**, *5* (43), 22472−22479.
(15) Zhang, H.; Wang, P.; Yang, J. Self-healing Epoxy via Epoxy−Amine Chemistry in Dual Hollow Glass Bubbles. *Compos. Sci. Technol.* **2014**, *94*, 23−29.
(16) Sun, D.; An, J.; Wu, G.; Yang, J. Double-layered Reactive Microcapsules with Excellent Thermal and Non-polar Solvent Resistance for Self-healing Coatings. *J. Mater. Chem. A* **2015**, *3*, 4435−4444.
(17) Kang, S.; Baginska, M.; White, S. R.; Sottos, N. R. Core−Shell Polymeric Microcapsules with Superior Thermal and Solvent Stability. *ACS Appl. Mater. Interfaces* **2015**, *7*, 10952−10956.
(18) Shchukin, D. G.; Sukhorukov, G. B.; Möhwald, H. Smart Inorganic/Organic Nanocomposite Hollow Microcapsules. *Angew. Chem., Int. Ed.* **2003**, *42*, 4472−4475.
(19) Patchan, M. W.; Fuller, B. W.; Baird, L. M.; Gong, P. K.; Walter, E. C.; Vidmar, B. J.; Kyei, I.; Xia, Z.; Benkoski, J. J. Robust Composite-Shell Microcapsules via Pickering Emulsification. *ACS Appl. Mater. Interfaces* **2015**, *7*, 7315−7323.
(20) Wang, T.; Wang, S.; Geng, L.; Fang, Y. Enhancement on Thermal Properties of Paraffin/Calcium Carbonate Phase Change Microcapsules with Carbon Network. *Appl. Energy* **2016**, *179*, 601−608.
(21) Tatiya, P. D.; Hedaoo, R. K.; Mahulikar, P. P.; Gite, V. V. Novel Polyurea Microcapsules Using Dendritic Functional Monomer: Synthesis, Characterization, and Its Use in Self-healing and Anticorrosive Polyurethane Coatings. *Ind. Eng. Chem. Res.* **2013**, *52*, 1562−1570.
(22) Yang, Z.; Hollar, J.; He, X.; Shi, X. A Self-healing Cementitious Composite Using Oil Core/Silica Gel Shell Microcapsules. *Cem. Concr. Compos.* **2011**, *33*, 506−512.
(23) Fujiwara, M.; Shiokawa, K.; Hayashi, K.; Morigaki, K.; Nakahara, Y. Direct Encapsulation of BSA and DNA into Silica Microcapsules (Hollow Spheres). *J. Biomed. Mater. Res., Part A* **2007**, *81A*, 103−112.
(24) Mandal, S.; Sathish, M.; Saravanan, G.; Datta, K. K. R.; Ji, Q.; Hill, J. P.; Abe, H.; Honma, I.; Ariga, K. Open-Mouthed Metallic Microcapsules: Exploring Performance Improvements at Agglomeration-Free Interiors. *J. Am. Chem. Soc.* **2010**, *132*, 14415−14417.
(25) Xu, J.; Ma, A.; Xu, Z.; Liu, X.; Chu, D.; Xu, H. Synthesis of Au and Pt Hollow Capsules with Single Holes via Pickering Emulsion Strategy. *J. Phys. Chem. C* **2015**, *119*, 28055−28060.
(26) Du, B.; Cao, Z.; Li, Z.; Mei, A.; Zhang, X.; Nie, J.; Xu, J.; Fan, Z. One-Pot Preparation of Hollow Silica Spheres by Using Thermosensitive Poly (N-isopropylacrylamide) as a Reversible Template. *Langmuir* **2009**, *25*, 12367−12373.
(27) Jeong, U.; Im, S. H.; Camargo, P. H. C.; Kim, J. H.; Xia, Y. Microscale Fish Bowls: A New Class of Latex Particles with Hollow Interiors and Engineered Porous Structures in Their Surfaces. *Langmuir* **2007**, *23*, 10968−10975.
(28) Tsuneyoshi, T.; Ono, T. Metal-Coated Microcapsules with Tunable Magnetic Properties Synthesized via Electroless Plating. *Mater. Sci. Eng. B* **2017**, *222*, 49−54.
(29) Patchan, M. W.; Baird, L. M.; Rhim, Y.-R.; LaBarre, E. D.; Maisano, A. J.; Deacon, R. M.; Xia, Z.; Benkoski, J. J. Liquid-Filled Metal Microcapsules. *ACS Appl. Mater. Interfaces* **2012**, *4*, 2406−2412.
(30) Hitchcock, J. P.; Tasker, A. L.; Baxter, E. A.; Biggs, S.; Cayre, O. J. Long-Term Retention of Small, Volatile Molecular Species within Metallic Microcapsules. *ACS Appl. Mater. Interfaces* **2015**, *7*, 14808−14815.
(31) Ma, Y.; Dong, W.-F.; Hempenius, M. A.; Möhwald, H.; Vancso, G. J. Redox-Controlled Molecular Permeability of Composite-Wall Microcapsules. *Nat. Mater.* **2006**, *5*, 724−729.
(32) Im, S. H.; Jeong, U.; Xia, Y. Polymer Hollow Particles with Controllable Holes in Their Surfaces. *Nat. Mater.* **2005**, *4*, 671−675.
(33) Li, W.; Matthews, C. C.; Yang, K.; Odarczenko, M. T.; White, S. R.; Sottos, N. R. Autonomous Indication of Mechanical Damage in Polymeric Coatings. *Adv. Mater.* **2016**, *28*, 2189−2194.
(34) Wang, Q.; Schlenoff, J. B. Single- and Multicompartment Hollow Polyelectrolyte Complex Microcapsules by One-Step Spraying. *Adv. Mater.* **2015**, *27*, 2077−2082.
(35) Hassander, H.; Johansson, B.; Törnell, B. The Mechanism of Emulsion Stabilization by Small Silica (Ludox) Particles. *Colloids Surf.* **1989**, *40*, 93−105.
(36) Jafari, S. M.; Assadpoor, E.; He, Y.; Bhandari, B. Re-coalescence of Emulsion Droplets During High-Energy Emulsification. *Food Hydrocolloids* **2008**, *22*, 1191−1202.

DOI: 10.1021/acsami.9b00827
ACS Appl. Mater. Interfaces 2019, 11, 9621−9628

(37) Fan, Y.; Simon, S.; Sjöblom, J. Chemical Destabilization of Crude Oil Emulsions: Effect of Nonionic Surfactants as Emulsion Inhibitors. *Energy Fuels* **2009**, *23*, 4575−4583.
(38) Balaraju, J. N.; Rajam, K. S. Preparation and Characterization of Autocatalytic Low Phosphorus Nickel Coatings Containing Submicron Silicon Nitride Particles. *J. Alloys Compd.* **2008**, *459*, 311−319.
(39) Pillai, A. M.; Rajendra, A.; Sharma, A. K. Electrodeposited Nickel−Phosphorous (Ni−P) Alloy Coating: An In-depth Study of Its Preparation, Properties, and Structural Transitions. *J. Coat. Technol. Res.* **2012**, *9*, 785−797.
(40) Krishnan, K. H.; John, S.; Srinivasan, K. N.; Praveen, J.; Ganesan, M.; Kavimani, P. M. An Overall Aspect of Electroless Ni-P Depositions—A Review Article. *Metall. Mater. Trans. A* **2006**, *37*, 1917−1926.
(41) Zhu, D. Y.; Rong, M. Z.; Zhang, M. Q. Self-healing Polymeric Materials Based on Microencapsulated Healing Agents: From Design to Preparation. *Prog. Polym. Sci.* **2015**, *49*−*50*, 175−220.
(42) Keller, M. W.; Sottos, N. R. Mechanical Properties of Microcapsules Used in a Self-healing Polymer. *Exp. Mech.* **2006**, *46*, 725−733.
(43) Yang, J.; Keller, M. W.; Moore, J. S.; White, S. R.; Sottos, N. R. Microencapsulation of Isocyanates for Self-Healing Polymers. *Macromolecules* **2008**, *41*, 9650−9655.

DOI: 10.1021/acsami.9b00827
ACS Appl. Mater. Interfaces 2019, 11, 9621−9628